Electrochemical characteristics of $Li_{2-x}VTiO_4$ rock salt phase in Li-ion batteries

R. Dominko [a,*], C. Vidal-Abraca Garrido [a], M. Bele [a], M. Kuezma [a], I. Arcon [b,c], M. Gaberscek [a,d]

[a] National Institute of Chemistry, Hajdrihova 19, SI-1000 Ljubljana, Slovenia
[b] University of Nova Gorica, Vipavska 13, SI-5000 Nova Gorica, Slovenia
[c] Jozef Stefan Institute, Jamova 39, SI-1000 Ljubljana, Slovenia
[d] Faculty of Chemistry and Chemical Technology, University of Ljubljana, Aškerčeva 5, 1000 Ljubljana, Slovenia

ARTICLE INFO

ABSTRACT

$Li_{2-x}VTiO_4$/C sample with a disordered rock salt structure was successfully prepared by annealing at a temperature of 850 °C. The electrochemical oxidation in the first cycle occurs at voltages above 4 V vs. metallic lithium, while the shapes of the electrochemical curves in consequent reduction–oxidation processes show a monotonous change of the potential between the selected cut-off voltages. A linear combination fit of individual XANES spectra was used for the determination of the oxidation states of as prepared sample and intermediate states during oxidation and reduction. In the as-prepared sample, vanadium was found to be in the average oxidation state of $V^{3.5+}$ and was additionally oxidized to $V^{3.8+}$ by the electrochemical charging. During the discharge process, the vanadium oxidation state was reduced to $V^{3.0+}$. In situ X-ray diffraction patterns and EXAFS analysis suggest good structural stability during oxidation and reduction, which is also reflected in the cycling stability if batteries were cycled in the voltage window between 2.0 V and 4.4 V. Extension of the lower cut-off voltage to 1.0 V doubles the capacity retention with the improved capacity stability if compared with several high capacity vanadium based materials.

1. Introduction

The demand for higher energy density lithium ion batteries is a constant driving force for the search of new materials and new systems. In terms of recent advances in the field, the positive electrode materials for Li-ion batteries can basically be divided into several different categories. Among those, the most promising seem to be certain mixtures of simple oxides $LiMO_2$ (M = Co, Ni, Mn,...) which can give capacities higher than 200 mAh g^{-1} [1], the use of oxygen from air as a cathode in Li-air batteries [2] and selected new compounds that can reversibly exchange more than 1 lithium per formula unit. An example of the latter are silicate-based positive materials with two lithium atoms per formula unit [3,4]; however, it is still not completely clear if in practice a >1 electron reaction is possible [5]. Another family of positive materials which theoretically enable a reversible exploration of more than 1 mol of lithium per formula unit are lithium transition metal oxides stabilized with titanium (so-called "titanates"). This family of positive materials with a general formula of Li_2MTiO_4 (M is transition metal) crystallize in a cubic rock-salt structure with considerable cation disorder [6–8]. The presence of Ti^{4+} in the structure and its strong bond with

O^{2-} enables the transition metals to be easily oxidized to a higher oxidation state [9]. On the other hand, vanadium-based positive materials are very well known to possess a high capacity [10–14]. Vanadium and titanium oxides $Li_2M_2O_4$ (M = V or Ti) with a rock salt structure were synthesized and tested by Thackeray's group more than two decades ago [15]. Thus, introducing vanadium as the transition metal M into the rock salt structure of the Li_2MTiO_4 family could be a reasonable attempt in the search for new materials with high reversible capacity. To the best of our knowledge, the only mixed vanadium–titanium oxide reported so far has been $LiVTiO_4$ with a spinel structure [12]. The main aim of the present study was to double the lithium content per formula unit, that is, to prepare and test a new active material with a formula Li_2VTiO_4 crystallized in disordered rock salt structure with an analogy to our previous studies [7,8].

2. Experimental

$Li_{2-x}VTiO_4$/C samples were prepared according to the procedure reported in our recent patent application [16]. Typically, 0.01 mol of TiO_2 was dispersed in 100 ml of deionized water using an ultrasonic processor where it was maintained after the addition of 0.02 mol lithium hydroxide. Separately, 0.005 mol of V_2O_5 was dissolved in 100 ml deionized water and 0.03 mol of citric acid was added. This mixture was maintained stirring overnight. Then, both solutions

* Corresponding author. Tel.: +386 14760362; fax: +386 14760422.
E-mail address: Robert.Dominko@ki.si (R. Dominko).

were mixed and the pH was adjusted to 7 by adding diluted NH_3 solution. After pH adjustment, the solution was dried at 60 °C. The xerogel was heat-treated in a gas-tight quartz tube in argon flow for 10 h at temperature at 850 °C (sample is labelled as LVT850).

Electrodes were prepared according to the standard procedure by mixing the active material (80 wt.%) with carbon black (10 wt.%) and an EPDM binder (10 wt.%) [7]. The electrodes were tested in a two-electrode vacuum-sealed triplex foil with a lithium metal as counter electrode. The electrodes in half cell were separated with a glass wool separator which was soaked with a 1 M solution of $LiPF_6$ in EC:DEC. The electrochemical characterization was performed on a VMP3 potentiostat/galvanostat at room temperature with a current density corresponding to C/10 and within different voltage windows.

Structural and crystallographic analyses of as prepared material were determined using a PANalytical X'pert PRO powder diffractometer. Evolution of the structural development with temperature was measured in a HTK1200 oven placed in the same diffractometer. For in situ XRD, as prepared LVT850 sample was used. Powder diffraction patterns were collected in a home-made cell on a Siemens D-5000 diffractometer in reflection (Bragg–Brentano) mode using Cu K_{α} radiation with Autolab cycling/data recording system. Data were collected in the range from 35° to 67° in steps of 0.04° and the integration time of 13 s per step. The cycling rate for LVT850 sample was C/50 with a cut-off voltage between 4.4 V and 1 V vs. metallic lithium. Each XRD scan corresponded to a compositional change of $\Delta x = 0.05$.

The surface morphology of the prepared composites was checked by a field emission scanning electron microscope (FE-SEM SUPRA 35VP, Carl Zeiss).

The carbon content was determined using TG analysis. The measurements were performed on a Mettler Toledo TGA/SDTA 851$_e$ thermoanalyzer in the temperature range from 30 up to 700 °C at a heating rate 10 °C min^{-1}.

In situ X-ray absorption experiment on the LVT850 sample, prepared in the form of half-battery were performed at room temperature in transmission detection mode at C beamline of HASYLAB at DESY. The total absorption thickness (μd) of the battery was of about 2 above the investigated V K-edge. A Si (1 1 1) double crystal monochromator was used with energy resolution of about 0.8 eV at V K-edge (5465 eV). Higher-order harmonics were effectively eliminated by detuning of the monochromator crystals to 60% of the rocking curve maximum, using the beam-stabilization feedback control. The intensity of the monochromatic X-ray beam was measured by three consecutive 10 cm long ionization detectors, respectively, filled with the following gas mixtures: 600 mbar N_2; 180 mbar Ar; 450 mbar Ar.

The half battery was mounted on a sample holder in the vacuum chamber between the first and the second ionization detector. The XAS spectra were measured initially on the as-prepared sample and repeated continuously during the first cycle. One spectrum was measured after the discharging at the end of first cycle. The current density used in in situ experiment was C/10. The measuring time for each spectrum was 34 min. In all, 25 XANES and EXAFS spectra were collected. XAS spectrum of the reference V compound (V_2O_5) was measured on the homogeneous pellet with the total absorption thickness of about 2 above the V K-edge. V_2O_5 sample was prepared from micronised powder homogeneously mixed with micronised BN powder.

The absorption spectra were measured within the interval [−250 to 1000 eV] relative to the V K-edge. In the XANES region equidistant energy steps of 0.25 eV were used, while for the EXAFS region equidistant k-steps ($\Delta k \approx 0.03$ Å^{-1}) were adopted with the integration time of 1 s/step. Exact energy calibration was established with the simultaneous absorption measurements on 5-μm thick V metal foil inserted between the second and third ionization

cell. Absolute energy reproducibility of the measured spectra was ±0.03 eV.

3. Results and discussion

While attempting to synthesize a $Li_{2−x}VTiO_4$/C material, we regularly observed a co-existence of two phases (a phase with a spinel structure and a phase with a disordered rock salt structure) during the synthesis. In order to modify the procedure with the aim to obtain the rock-salt pure phase (or at least as pure as possible), we decided to monitor carefully the structural evolution during the synthesis. Specifically, we have performed in situ thermal treatment in a HTK1200 chamber attached to an X-ray diffractometer. A 2:1:1 mixture of the initial Li:V:Ti precursors was used in the experiment. The evolution of XRD patterns during the heat treatment is shown in Fig. 1a. The obtained XRD patterns can be divided into three different temperature regions. From 25 °C up to 400 °C only the diffraction peaks from the precursors are observed. Above 400 °C, the evolution of diffraction peaks that correspond to the formation of the spinel phase, i.e., Li_yVTiO_4 appear and reach a max-
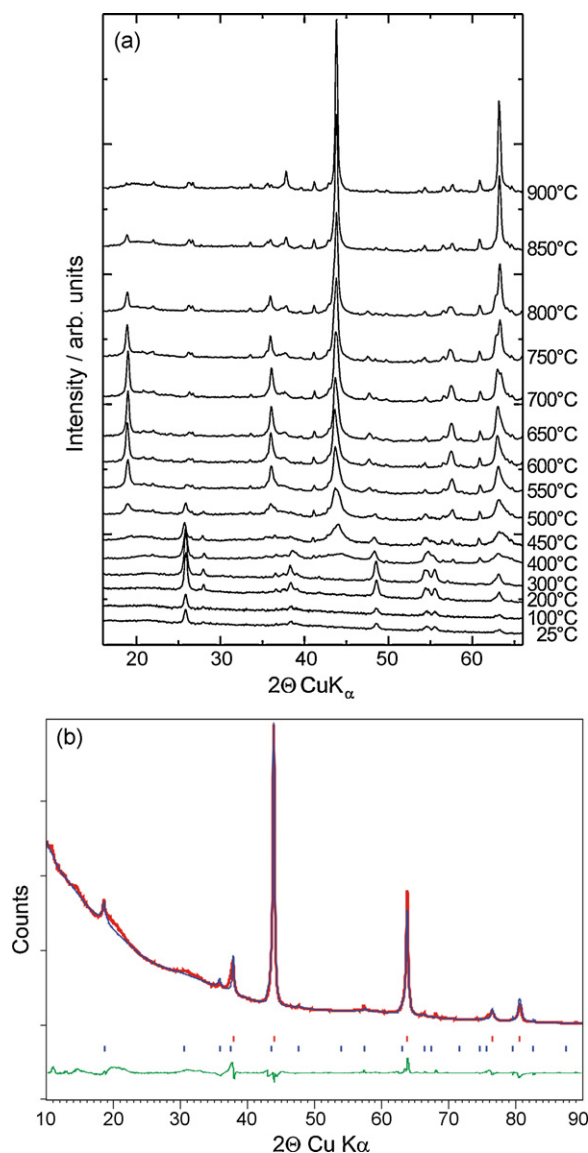

Fig. 1. (a) Evolution of the structure during the heating of initial precursor mixture as measured with an in situ high-temperature XRD. (b) Refinement for the XRD pattern obtained from LVT850 sample.

imum intensity at about 700 °C. Above 700 °C, the spinel phase is being transformed into the rock salt phase. Thus, at temperatures between 850 °C and 900 °C only a small fraction of the remaining spinel phase is detected. A similar phase transition (spinel to rock salt) was observed previously by De Picciotto and Thackeray [15] in $Li_{1+x}V_2O_4$ and ascribed to the change of relative energies of the 8a and 16c sites during the transformation from one to the other structure.

In all our further attempts to synthesize crystallographically pure rock salt phase (variation of the heat treatment parameters, changing the starting composition) we have always ended up with co-existence of the two phases. The purest sample with (predominantly) rock salt structure has been synthesized from precursors having a ratio of Li:V:Ti = 2:1:1 and using a heat treatment up to 850 °C with subsequent slow cooling down to room temperature (this sample is labelled in continuation as LVT850). Fig. 1b shows a refinement of the XRD spectrum of the LVT850 sample. Co-existence of a major rock-salt and a minor spinel structures have been detected. The contribution of rock salt phase was fitted within the $Fm3m$ space group while the contribution of spinel phase was fitted with the $Fd\bar{3}m$ space group. The refined room temperature cell parameters are $a = b = c = 4.140(2)$ Å and $a = b = c = 8.353(6)$ Å for the rock salt and the spinel phase, respectively. The agreement factors were $R_p = 3.25(1)$ % and $R_{wp} = 5.12(8)$ %, respectively.

The morphology of active phase, as well as of other electrode components, and the particle size of the as-prepared $Li_{2-x}VTiO_4$/C composite can be tuned by the amount of organic phase used in the synthesis. Addition of citric acid as a chelating agent and as a source of in situ carbon leads to the formation of homogenously distributed particles in a porous carbon matrix. In our previous works [17,18] we showed that degradation of citric acid leads to the porous composite with a residue carbon which can act as a electron conductive coating (matrix) on active particles. The carbon content in the sample used in this study was 12.4 wt.%. Particle size distribution is narrow (Fig. 2) with an estimated d_{50} diameter of particles was between 40 and 60 nm (Fig. 2a). As-prepared composites show a high degree of porosity (Fig. 2b), which is essential for the optimal electrochemical behaviour of Li_2MTiO_4 (M = Fe, Mn, Ni) positive materials [7].

LVT850 sample with a predominant rock-salt phase composition was electrochemically characterized using standard approaches when testing new materials. Namely, to the best of our knowledge the electrochemical properties of $Li_{2-x}VTiO_4$ with a rock-salt structure has not been published up to date, while the electrochemical properties of $LiVTiO_4$ with a spinel structure were shown in the contribution by Baker et al. [12]. The galvanostatic cycling tests were performed in three different voltage windows: a narrow electrochemical window between 2.0 V and 4.2 V (Fig. 3a), an extended electrochemical window between 2.0 V and 4.4 V (Fig. 3b) and a wide electrochemical window between 1.0 V and 4.4 V (Fig. 3c) vs. metallic lithium. In all three cases, we have found that, during the first oxidation, the electrochemical curve possesses a different shape than in higher cycles (later oxidation/reduction processes). Specifically, the first oxidation process takes place mainly at voltages above 4.0 V vs. metallic lithium, whereas in higher cycles the shape of the electrochemical curve shows a monotonous change of the potential between the selected cut-off voltages. The major difference between the three different voltage limits is in the obtained capacity (Fig. 3d). Furthermore, one can also observe that the polarisation between the charge and discharge curve becomes larger when a wider electrochemical window is used. While the origin of higher capacity can probably be explained by a change in the redox oxidation state of vanadium, the origin of higher polarisation is not clear at the present state of research. Besides in the formation cycles where discharge capacity is higher compared to charge capacity, the columbic efficiency is
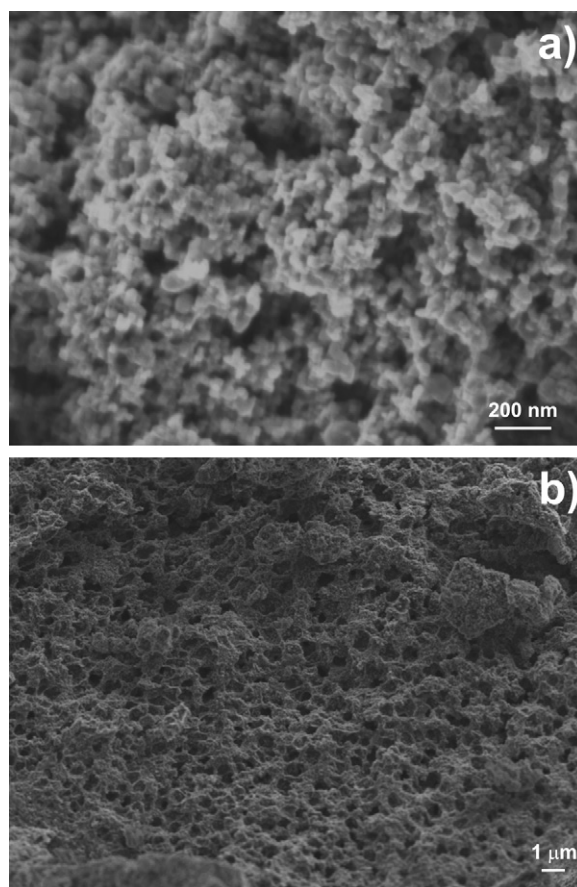

Fig. 2. (a) and (b) SEM micrographs of LVT850 sample at low and high magnification.

close to above 95% (Fig. 3d—open symbols). The capacity retention in the formation cycles suggests good cyclability of the proposed samples when the cut-off voltage of 2.0 V vs. metallic lithium is used. The theoretical capacity for the exchange of 1 mol of lithium is 164.6 mAh g^{-1}. A capacity close to this value can be obtained if the samples are cycled with the lower cut-off voltage limit of 2.0 V. Extending this limit to 1.0 V vs. lithium metallic reference almost doubles the capacity. Importantly, this very high capacity of about 300 mAh g^{-1} remains quite stable at least during further 15 cycles (Fig. 3d—triangles). It can be concluded that the cycling stability of LVT850 is considerably better if compared to several other high-capacity vanadium-based materials, where up to 30% of the capacity may be lost within first 10 cycles [19–21].

The structural stability in the first cycle was checked by a combination of the electrochemical and X-ray diffraction methods. A low current density corresponding to a cycling rate of C/50 and the wide electrochemical window were used in this experiment. The charge used during the first oxidation process was slightly higher than the charge needed for the removal of one mol of lithium, while the charge used during the first reduction process was approximately equal to the insertion of 1.4 mol of lithium. During this oxidation–reduction process the lattice parameters of the LVT850 sample undergo relatively small changes. Such a continuous change of Bragg positions of peaks with increasingly exchanged amount of lithium is typical for the solid solution exchange mechanism (Fig. 4a). The small and continuous changes in the position of diffraction peaks after oxidation and reduction process in the first cycle may reflect quite good structural stability of the LVT850 material. However, a more detailed comparison of X-ray diffraction patterns at the beginning and at the end of the oxidation/reduction cycle reveals that the position of [2 2 2] peak after the reduction is
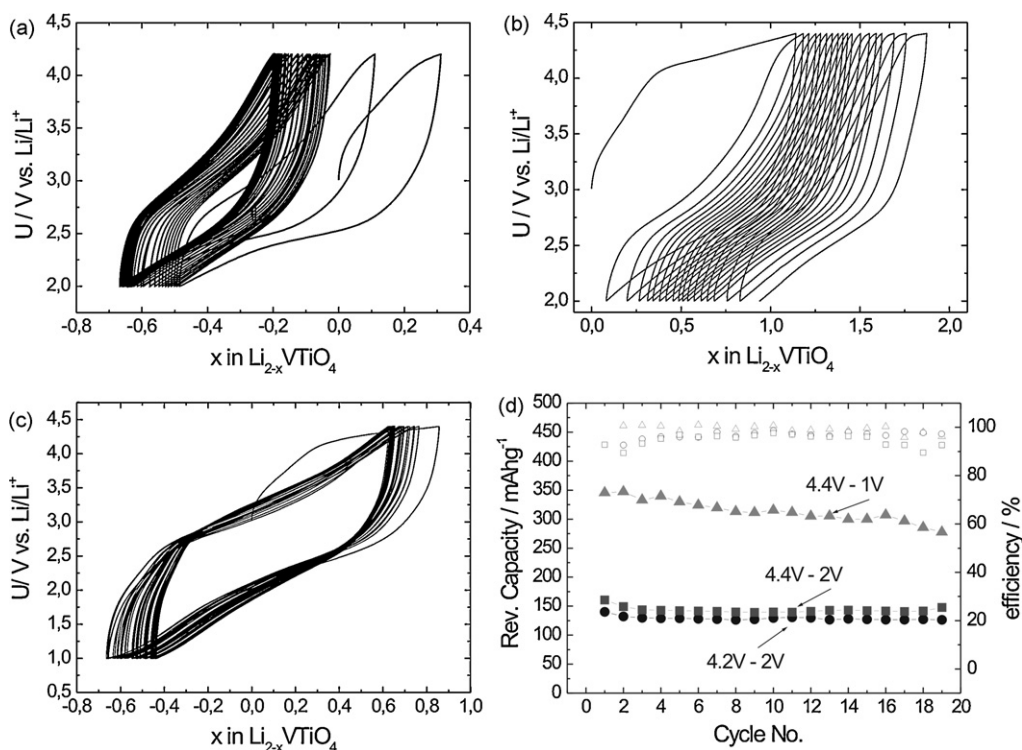
Fig. 3. (a–c) Cycling behaviour of LVT850 sample in the three different electrochemical windows obtained with C/10 cycling rate at room temperature: between 2 V and 4.2 V (a), between 2 V and 4.4 V (b), and between 1 V and 4.4 V (c). Cycling performance of LVT850 sample cycled within three different voltage windows (reversible capacity—filled symbols and cycling efficiency—open symbols) (d).
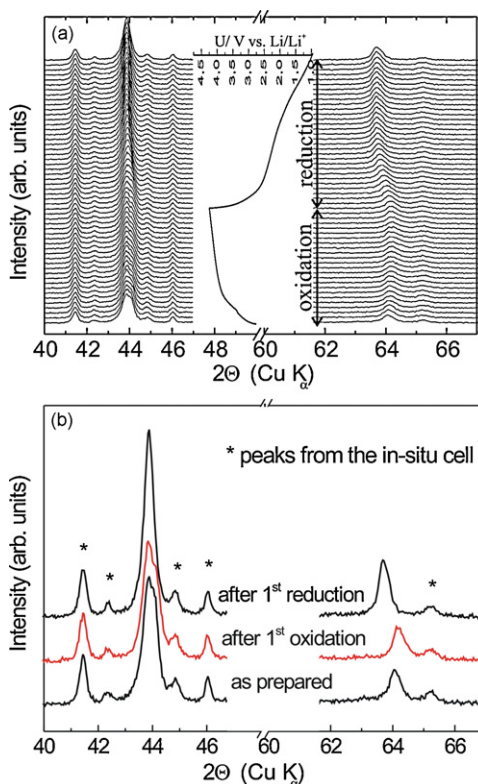

Fig. 4. Voltage limited in situ X-ray diffraction experiment on LVT850 sample: (a) obtained X-ray diffraction patterns during oxidation/reduction process combined with an electrochemical curve during the experiment (left column shows the shift of [0 0 2] peak and right column shows the shift of [2 2 2]); (b) selected X-ray diffraction patterns showing [0 0 2] and [2 2 2] peaks of as prepared; oxidized and reduced phases.

not at the same position when compared to as-prepared sample (Fig. 4b). It is shifted from $2\theta = 64.04°$ to $2\theta = 64.16°$ during first oxidation and back to $2\theta = 63.68°$ during the first reduction. A lower 2Θ value (higher cell volume) suggests that more lithium was inserted into the cell compared to as prepared material.

3.1. X-ray absorption spectroscopy

Direct insight into the change of the oxidation state and local symmetry of vanadium was obtained by in situ X-ray absorption spectroscopy. The V K-edge XANES is used to monitor the change of V valence state during the charge/discharge process. The analysis of XANES spectra was performed with the IFEFFIT program package ATHENA [22]. Fig. 5a shows the normalized V XANES spectra of samples at representative times in the process of charging and discharging, and the reference compounds that were extracted by a standard procedure [23].

The shape of the edge and the pre-edge region resonances are characteristic for the local symmetry of vanadium sites and their energy positions are correlated with the valence state of V atoms. Octahedrally coordinated vanadium cations that possess an inversion center (for example in VO), exhibit a weak triplet resonance structure in the pre-edge region [23]. On the other hand, vanadium cations located at sites without an inversion center (for example tetrahedrally coordinated in $CrVO_4$, square pyramidal in V_2O_5, or distorted octahedrally coordinated in V_2O_4) exhibit a characteristic isolated pre-edge peak [23,24]. In our case, all XANES spectra of the sample exhibit very similar edge profiles with a pre-edge resonance, characteristic of V cations lacking an inversion center (distorted octahedral coordination).

With increasing oxidation state each absorption feature in the XANES spectrum is shifted to higher energies. Shift of the V edge to higher energies is observed during battery charging (oxidation), indicating oxidation of V, and in the process of discharging (reduc-
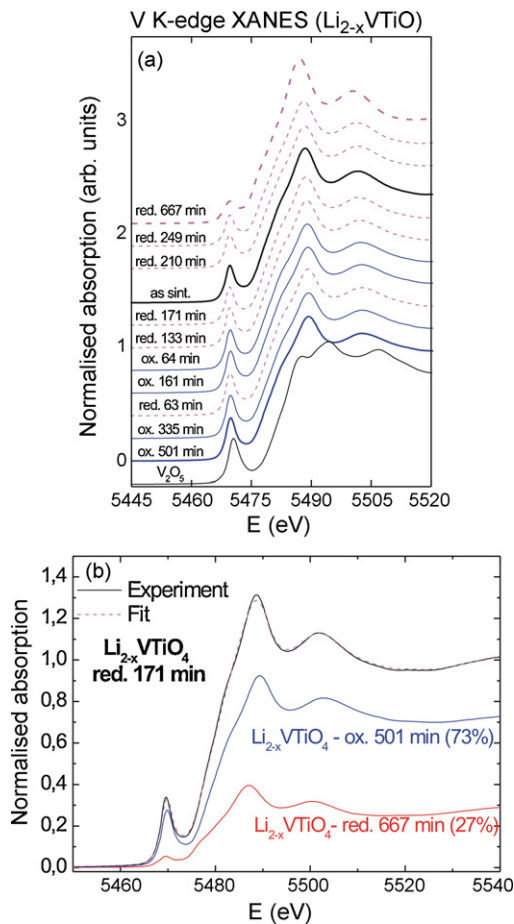
Fig. 5. (a) The V K-edge XANES spectra of $Li_{2-x}VTiO_4$ sample during the oxidation and reduction, and V_2O_5 reference compound. The spectra are displaced vertically for clarity. (b) V K-edge XANES spectrum of Li_2VTiO_4 sample after 171 min of reduction: Solid line—experiment; magenta dashed line—best-fit linear combination of XANES profiles of Li_2VTiO_4 sample after 667 min of reduction ($V^{3.0+}$) and after 501 min of oxidation ($V^{3.8+}$) (both components are shown below). (For interpretation of the references to color in this figure legend, the reader is referred to the web version of the article.)

Fig. 6. The relative amount of V^{4+} component in the $Li_{2-x}VTiO_4$ positive material during the first cycle of charge/discharge process, determined from V XANES spectra (left axis) and corresponding electrochemical curve obtained during in situ measurement (right axis).

tion), gradual shifts of the edge to lower energies indicates the reduction of V. The edge position after reduction is at significantly lower energy compared to that in the as-synthesized sample, which clearly shows that average vanadium valence state after reduction in the first cycle is lower than in the as prepared material.

A linear relation between the edge shift and the oxidation state was established for V atoms in different vanadium oxides: the absorption edge shifts for 2.5 eV per valence [23]. However, different local environments of the cation result in different K-edge profiles. The comparison of the edge shift in such cases is hindered [24]. If the sample contains the same cation in two or more sites with different local structures and valence states, the measured XANES spectrum is a linear combination of individual XANES spectra of the different cation sites. In such cases the relative amounts of the cation at each site can be precisely determined by the linear combination fit [8,25]. The procedure is applied to V XANES spectra measured during the charge/discharge process. The XANES spectra of intermediate states can be very well described by the linear combination of the XANES spectrum of the final Li_2VTiO_4 state after battery discharging, and the spectrum at the highest average vanadium oxidation state, obtained after complete charging. An example of the fit result is illustrated in Fig. 5b. In this way we were able to determine the relative amount of each component in all intermediate states with a precision of 1% or better.
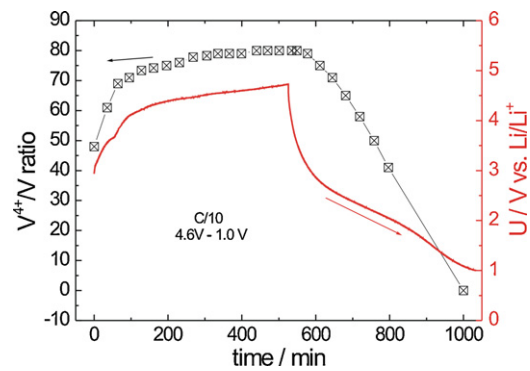
To deduce the average V valence state in the intermediate states the average V valence in both limiting states need to be determined independently. For the purpose a comparison of the V edge energy with reference vanadium compounds with a similar composition and similar local symmetry of V atom neighbourhood is used. The edge position (defined as the second maximum in the edge derivative spectrum) in the final $Li_{2-x}VTiO_4$ state after battery discharging coincides with that in reference V_2O_3, where V is trivalent. Taking into account edge shifts of 2.5 eV per valence, we estimate the average valence of V in the most oxidized state after charging to be $V^{3.8+}$. The uncertainty in the determination of the average V valence of these two limiting states is about $\pm 5\%$.

The XANES results therefore show that during battery oxidation the average vanadium valence is gradually increased from $V^{3.5+}$ to $V^{3.8+}$. During reduction the average V valence gradually decreases to its final value of $V^{3.0+}$. The relative amount of V^{4+} valence state during the first cycle of charging and discharging of the battery is plotted in Fig. 6 (assuming that only V^{3+} and V^{4+} cations are present). In the particular in situ experiment the change of vanadium oxidation state does not follow the charge passed through the electrochemical cell during the first oxidation process, while it is in the agreement with a change of oxidation state of vanadium during the reduction process. No change in the oxidation state and in the local environment of titanium has been detected at the end of the reduction, when compared with as prepared sample. The oxidation state of vanadium in the as prepared sample ($V^{3.5+}$) suggests that $Li_{2-x}VTiO_4$ sample is at least partially oxidized and this explains the anomaly observed during the cycling where we observed higher discharge capacity compared to charge capacity in the first cycle (see Fig. 3). Under specific conditions for in situ XAS experiment (battery was cycled in the vacuumed chamber) we reached oxidation state of vanadium $V^{3.0+}$ at the end of reduction. In the future additional experiments should be performed if fully lithiated Li_2VTiO_4 sample can be prepared with vanadium in the oxidation state V^{2+} and if observed capacities above 300 mAh g^{-1} can be correlated to the change of the oxidations state of vanadium from V^{2+} to V^{4+}.

Vanadium K edge EXAFS analysis is used to directly probe the changes in the short range order around V cations in the $Li_{2-x}VTiO_4/C$ positive material during oxidation and reduction. Fourier transforms of the representative EXAFS spectra from the series obtained during first charge/discharge cycle are shown in Fig. 7, revealing the contributions of individual shells of atoms around V. All the spectra in the series are very similar, indicating that the local environment around V cations does not change significantly during the process of oxidation and reduction in the first cycle.
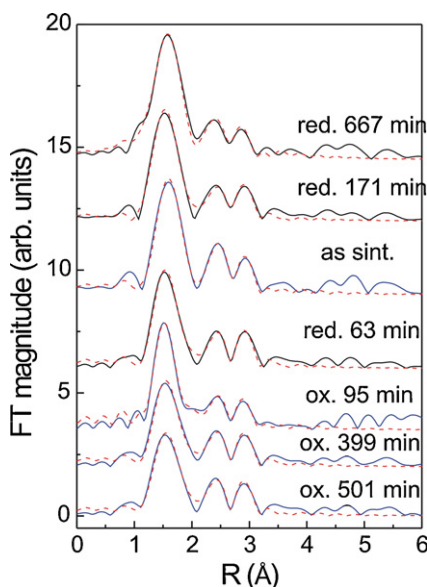
Fig. 7. Fourier transform of k^3-weighted V EXAFS spectra of $Li_{2-x}VTiO_4$ sample during the process of oxidation and reduction, calculated in the k range of 4–14 $Å^{-1}$. Experiment—solid line; EXAFS model—dashed line.

In order to obtain quantitative structural data from the series, we modelled the spectra with an *ab initio* FEFF model [26]. The basic model is built with the help of crystallographic data of $Li_{2-x}VTiO_4$ with $Fm3m$ space group. In this rock-salt crystal structure V atoms are located at the centers of oxygen octahedra. The second coordination shell is occupied by six Li, three V and three Ti atoms at the same distance. The third coordination shell is composed of eight O atoms. The quantitative analysis of V EXAFS spectra is performed with the IFEFFIT program package [2⁰]. Structural parameters are quantitatively resolved by comparing the measured signal with model signal in the best fit procedure. The model includes all neighbour shells described above, comprising four single-scattering paths with lengths up to 3.7 Å. In addition, a deviation from the basic rock-salt structure is introduced artificially into the FEFF model by replacing the single 6-fold degenerate V–O scattering path with two paths with different V–O distances and relative number of oxygen atoms at each distance, to describe the deformation of the octahedron. Similar deformation is allowed in the model of the second coordination shell for V and Ti neighbours. Distances and Debye–Waller parameters for each path are varied, and a common shift of energy origin ΔE_o. The stoichiometry, however, is not varied: the degeneracy of individual scattering paths is left as defined from the crystallographic data, except for the amount of Li atoms, which is adjusted to the extent lithium extraction or insertion. The EXAFS amplitude reduction factor S_0^2 is kept fixed at the value of 0.80.

The model fits very well all the measured EXAFS spectra in the series in the k range of 4 $Å^{-1}$ to 14 $Å^{-1}$, and R range of 1–3.5 Å. Obtained structural parameters confirm that there are no significant changes of local structure during charging and discharging. In all cases the local structure around V is found to be deformed, compared to that in the rock-salt crystal structure. In the final state, after reduction we found one oxygen atom at a short distance of 1.79 Å and five oxygen atoms at 2.01 Å. In the second coordination shell there are six Li atoms at 2.9 Å, three V or Ti atoms at 2.91 Å and three V or Ti atoms at 3.10 Å. Next coordination shell contains eight oxygen atoms at 3.75 Å. The ambiguity in second shell composition (Ti or V) is due to the fact that neighbours with close atomic numbers as V and Ti cannot be unambiguously distinguished by EXAFS spectroscopy. Most probably, the two ele-

ments randomly occupy both positions in the second coordination shell.

To conclude, the local structure around V atoms in the positive material is very rigid and does not change significantly in the process of lithium extraction and insertion. That analysis confirms the structural stability observed by in situ XRD.

4. Conclusions

We have synthesized novel positive material $Li_{2-x}VTiO_4$/C with a disordered rock-salt structure. Co-existence of the rock-salt and spinel type of the phases was found during the synthesis in the temperature range from 550 °C to 900 °C. However, at higher temperatures the presence of the rock-salt prevails. The electrochemical tests show good cycling stability in the voltage windows between 2.0 V and 4.4 V vs. metallic lithium with a capacity close to the theoretical value for 1 electron reaction. In a wider potential window, i.e., between 4.4 V and 1.0 V vs. lithium reference, the capacity was doubled and a starting reversible capacity close to 350 mAh g^{-1} has been obtained. An in situ X-ray diffraction experiment has suggested a good structural stability with the increase of the cell volume after completed reduction when compared to the one in the as-prepared sample. That was explained by in situ X-ray absorption spectroscopy, with which we determined the average oxidation state of vanadium in the as prepared sample to be $V^{3.5+}$. During the first oxidation we detected a small increase of the oxidation state of vanadium which was smaller compared to the charge used for the electrochemical oxidation, while during the first reduction process the change of oxidation state of vanadium was in the agreement with a charge used for the electrochemical reduction. In situ V K-edge EXAFS analysis suggests rigid local environment around vanadium in the structure during oxidation/reduction processes.

References

[1] T. Ohzuku, Y. Makimura, Chem. Lett. 7 (2001) 642–643.
[2] T. Ogasawara, A. Debart, M. Holzapfel, P. Novak, P.G. Bruce, J. Am. Chem. Soc. 128 (2006) 1390–1393.
[3] A. Nyten, A. Abouimrane, M. Armand, T. Gustafsson, J.O. Thomas, Electrochem. Commun. 7 (2005) 156–160.
[4] R. Dominko, M. Bele, M. Gaberscek, A. Meden, M. Remskar, J. Jamnik, Electrochem. Commun. 8 (2006) 217–222.
[5] Z.L. Gong, Y.X. Li, Y. Yang, Electrochem. Solid-State Lett. 9 (2006) A542–A544.
[6] L. Sebastian, J. Gopalakrishnan, J. Solid State Chem. 172 (2003) 171–177.
[7] M. Kuezma, R. Dominko, A. Meden, D. Makovec, M. Bele, J. Jamnik, M. Gaberscek, J. Power Sources 189 (2009) 81–88.
[8] M. Kuezma, R. Dominko, D. Hanzel, A. Kodre, I. Arcon, T. Meden, M. Gaberscek, J. Electrochem. Soc. 156 (2009) A809–A816.
[9] S.R.S. Prabaharan, M.S. Michael, H. Ikuta, Y. Uchimoto, M. Wakihara, Solid State Ionics 172 (2004) 39–45.
[10] L.A. De Picciotto, M.M. Thackeray, Solid State Ionics 18–19 (1986) 773–777.
[11] Y. Wang, G. Cao, Adv. Mater. 20 (2008) 2251–2269.
[12] J. Baker, M.Y. Saidi, J.L. Swoyer, Solid State Ionics 167 (2004) 413–418.

[13] N. Ding, X. Feng, S. Liu, J. Xu, X. Fang, I. Lieberwirth, C. Chen, Electrochem. Commun. 11 (2009) 528–541.
[14] D. Guy, B. Lestriez, D. Guyomard, Adv. Mater. 16 (2004) 541–553.
[15] L.A. De Picciotto, M.M. Thackeray, Solid State Ionics 28–30 (1988) 1364–1370.
[16] M. Bele, R. Dominko, C. Vidal-Abraca Garrido, M. Pivko, M. Gaberscek, Patent Application P-200900248, Slovenia (2009).
[17] R. Dominko, M. Bele, J.-M. Goupil, M. Gbaerscek, D. Hanzel, I. Arcon, J. Jamnik, Chem. Mater. 19 (2007) 2960–2969.
[18] J. Moskon, R. Dominko, M. Gaberscek, R. Cerc-Korosec, J. Jamnik, J. Electrochem. Soc. 153 (2006) A1805–A1811.
[19] S. Jouanneau, A. Verbaere, S. Lascaud, D. Guyomard, Solid State Ionics 3–4 (2006) 311–315.
[20] S. Jouanneau, A. Verbaere, D. Guyomard, J. Solid State Chem. 172 (2003) 116–122.
[21] H. Yang, J. Li, X.-G. Zhang, Y.-L. Jin, J. Mater. Process. Technol. 1–3 (2008) 265–270.
[22] B. Ravel, M. Newville, J. Synchrotron Radiat. 12 (2005) 537.
[23] J Wong, F.W. Lytle, R.P. Messmer, D.H. Maylotte, Phys. Rev. B 30 (1984) 5596–5610.
[24] C. Rossignol, G. Ouvrard, E. Baudrin, J. Electrochem. Soc. 148 (2001) A869–A877.
[25] R. Dominko, I. Arcon, A. Kodre, D. Hanzel, M. Gaberscek, J. Power Sources 189 (2009) 51–58.
[26] J.J. Rehr, R.C. Albers, S.I. Zabinsky, Phys. Rev. Lett. 69 (1992) 3397–3400.